

1 **Probabilistic Design and Reliability Analysis of Scour Protections for Offshore**
2 **Windfarms**

3
4 **T. Fazerer-Ferradosa^{1*}, F. Taveira-Pinto¹, X. Romão¹, E. Vanem²,**
5 **M. T. Reis³, L. das Neves^{1,4}**

6
7 ¹Department of Civil Engineering, Faculty of Engineering, University of Porto (FEUP),
8 Rua Dr. Roberto Frias, Campus FEUP, 4200-465 Porto, Portugal.

9 ²DNV-GL Strategic Research and Innovation, Department of Mathematics, University of Oslo,
10 Høvik and Oslo, Norway.

11 ³Hydraulics and Environment Department, National Laboratory for Civil Engineering (LNEC),
12 Av. do Brasil 101, 1700-066, Lisbon, Portugal.

13 ⁴International Marine and Dredging Consultants (IMDC), Van Immerseelstraat 66
14 B-2018, Antwerp, Belgium.

15
16
17
18 *Corresponding author: dec12008@fe.up.pt
19
20
21
22
23
24
25
26
27
28
29
30
31
32
33
34

ABSTRACT

Scour protection is an important component of fixed bottom foundations for offshore wind turbines. Depending on the hydrodynamic conditions, they might be indispensable to avoid the structural collapse of the foundation due to scour phenomena. The design of scour protections is typically deterministic, which often results in overestimated mean diameters of the armour layer. Moreover, the design methodologies currently applied do not provide a measure of safety associated with the proposed design. The present research proposes a novel methodology to assess the safety of the protection and to perform the probabilistic design of static and dynamic scour protections. A case study based on Horns Rev 3 offshore wind farm is used to show how to select the mean stone diameter according to a pre-defined probability of failure of the protection. The results show that a dynamic scour protection could be safely designed with a reduction of the mean stone diameter up to 15 cm, when compared with the statically stable protection.

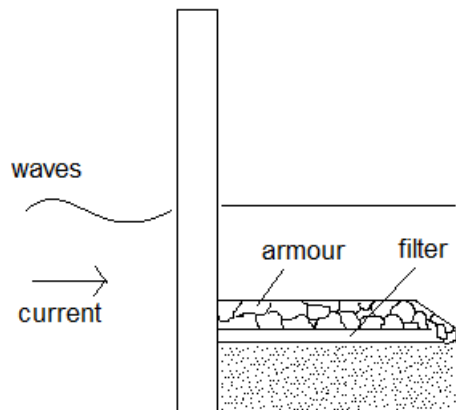
KEYWORDS: Scour Protection, Probabilistic Design, Offshore Wind Turbines, Optimisation, Reliability, Probability of Failure.

51 **1. INTRODUCTION**

52

53 The majority of offshore wind turbines with fixed-bottom foundations are based on monopile
54 foundations, i.e. about 81% of the installed substructures [1]. These fixed foundations are often
55 subjected to scour phenomena, which may lead to structural problems related to loss of moment
56 bearing capacity and fatigue induced instability [2]. Scour phenomena may also lead to
57 significant changes in the natural frequency of the wind turbine. In order to mitigate scour
58 phenomena, one may use a scour protection which typically consists of a filter layer and rock
59 material placed around the monopile to avoid the general loss of sand-bed material [3], as
60 shown in Figure 1.

61



62

63

Figure 1. Scour protection with armour and filter layer

64

65 A major aspect of scour protection design is the definition of the mean diameter of the stones
66 (D_{50}) of the armour layer placed above the filter [4]. Scour protections are typically designed in
67 a deterministic way, mainly based on empirical methodologies that account for the wave and
68 current induced bed shear stress, which may drag the armour stones and eventually, lead to the
69 erosion of the scour protection and the soil around the foundation, e.g. [5], [6] and [7] .

70 The foundation of an offshore wind turbine roughly corresponds to 30% of the overall cost (e.g.
71 see [8] or [9]) and an important part of those costs is related to the scour protection. Therefore,
72 several works have been performed aiming at optimising the mean stone diameter, e.g. [10],
73 [11] and [12] tried to improve cost-benefit ratios of the scour protection by means of a
74 reduction in the D_{50} . One of the most recent optimisation methods consists in designing a
75 dynamic scour protection, instead of the static one, commonly used in the industry, e.g. [13]
76 and [14].

77 In static scour protections, the top layer stones are not allowed to move. This means that the
78 mean diameter of the stones is defined so that, for a specific weight of the rock material, the
79 wave- and current-induced shear stress in the foundation's vicinity is not enough to overcome
80 the critical shear stress of the stones [6]. The critical shear stress defines the threshold of
81 motion, i.e. the minimum shear stress necessary to drag the stones from their initial position
82 [5]. In this sense, the failure of a static scour protection is considered to occur when there is
83 movement of the armour stones.

84 Alternatively, dynamic scour protections allow for a certain degree of movement of the armour
85 stones, without exceeding a maximum exposed area of the filter layer defined by [10] and [14]
86 as $4D_{50}^2$. Allowing for some movement of the stones enables one to reduce the mean diameter,
87 because there is no need to ensure that the acting shear stress is not equal or larger than the
88 critical one. Dynamic scour protections were extensively studied in [3], which introduced a
89 design criterion based on the dimensionless damage number (S_{3D}). The damage number
90 provides a measure of the damage expected to occur in the protection for specific
91 hydrodynamic conditions and the mean diameter used. Moreover, [14] conducted a large series
92 of scour tests, based on a physical model of a monopile foundation at a scale of 1:50 (with
93 Froude similitude) and concluded that dynamic scour protections could be obtained for $S_{3D} \leq 1$.
94 The feasibility of dynamic scour protections was later confirmed by [12] and [15], using a
95 similar physical model that encompassed a larger range of the mean stone diameter.

96 However, despite the optimisations proposed in the literature, the reliability and failure analysis
97 of static and dynamic scour protections have not been extensively addressed. Performing the
98 failure analysis of scour protections not only enables quantifying the safety level of the
99 protection, but it also enables one to perform a probabilistic design, which may solve the
100 problem of the uncertainty and overestimated mean diameters that come from deterministic
101 methodologies. In this paper, a case study utilizing in met-ocean data from the Horns Rev 3
102 offshore windfarm is used to perform the reliability assessment of a scour protection designed
103 according to deterministic methodologies. Furthermore, a novel probabilistic design method is
104 proposed for static and dynamic scour protections. The new methodology is based on Monte-
105 Carlo simulations combined with the failure criteria proposed in [6] and [14], and provides the
106 mean stone diameter of the scour protection for a pre-defined probability of failure.

107 This paper is a contribution to the very few existent studies concerning the maritime
108 environment and the failure of the protection itself, e.g. [11]. Hence, this paper aims to

109 contribute to optimise the design of the protections, under waves and currents combined, by
110 means of failure analysis.

111

112 **2. DETERMINISTIC DESIGN AND FAILURE OF SCOUR PROTECTIONS**

113 The traditional design of scour protections implies the definition of several parameters of the
114 protection, e.g. the thickness of the filter and the armour layer, the extent of the protection and
115 mean diameter of the rock material (i.e. D_{50}). The present research is focused on the latter,
116 which must be designed to avoid erosion of the armour layer. There are several deterministic
117 methodologies to determine the value of D_{50} , e.g. [16], [17], [18] or [19]. The current paper is
118 focused on the methodologies defined in [20], due to its wide use and simplicity and in [6] and
119 [14], which correspond to optimised design approaches for static and dynamic scour
120 protections, respectively. For further details on the methodologies applied in this paper, one
121 refers to [3].

122

123 *2.1 Static scour protections*

124 As previously stated the design of statically stable scour protections generally involves the
125 assessment of the bed shear stress induced by the combined effect of waves and currents (τ_{wc}).
126 If the protection is intended for static stability, the armour stones are not allowed to move.
127 Hence, the stones placed in the armour layer must be large enough to ensure that their critical
128 shear-stress (τ_{cr}) is higher than the bed shear stress acting on the protection [21], including the
129 effect of the monopile's presence [20].

130 In order to account for the monopile's presence, the amplification factor (α) is typically
131 employed. The amplification factor is defined as the ratio of the undisturbed bed shear-stress to
132 the increased shear-stress in the presence of a structure, in this case the monopile foundation.
133 The amplification factor may vary depending on the hydrodynamic condition. According to
134 [14], physical model studies show that for waves alone α varies between 2.2 and 2.5, but when
135 the effect of currents is included one commonly uses α equal to 4. Note, however, that the
136 amplification factor may be larger depending on the case, e.g. [5] and [18] report other
137 situations where α is larger than 4, e.g. for monopiles under waves and current combined.

138 One of the problems of dealing with waves and currents combined lies in obtaining the
139 maximum bed shear stress caused by their simultaneous action (τ_{wcmax}). In current practice, one
140 of the most widely used methodologies used to obtain τ_{wcmax} , due to its simplicity and accuracy
141 is the one presented by [20], which is also discussed in [22] and adapted to account for non-

142 linear effects in [23]. In order to perform the deterministic design of a scour protection
 143 according to [20] the critical shear stress can be defined by Eq.1.

144

$$145 \quad \tau_{cr} = g(\rho_s - \rho_w)D_{50}\theta_{cr} \quad (1)$$

146

147 where g is the gravitational acceleration, ρ_w is the water density, ρ_s is the density of the rock
 148 material and θ_{cr} is the non-dimensional critical Shields parameter as introduced in [21]. As
 149 showed in [6] for sufficiently large non-cohesive sediments, one can use $\theta_{cr}=0.056$. Then the
 150 maximum shear stress, under waves and currents combined, can be assessed according to Eq. 2,
 151 where τ_m is the mean combined bed shear-stress (Eq. 3), τ_w is the wave-induced bed shear
 152 stress, τ_c is the current-induced bed shear-stress and ϕ is the angle between waves and currents
 153 [20]:

154

$$155 \quad \tau_{wc\max} = \left[(\tau_m + \tau_w \cos \phi)^2 + (\tau_w \sin \phi)^2 \right]^{1/2} \quad (2)$$

156

$$157 \quad \tau_m = \tau_c \left[1 + 1.2 \left(\frac{\tau_w}{\tau_c + \tau_w} \right)^{3.2} \right] \quad (3)$$

158

159 The design value of D_{50} is the minimum value that complies with Eq. 4, which depends on the
 160 selected amplification factor (α).

161

$$162 \quad \tau_{cr} > \alpha \times \tau_{wc\max} \quad (4)$$

163

164 In a similar way, an optimisation for statically stable scour protections was proposed by [6],
 165 which introduces an alternative formula (Eq. 5) for $\tau_{wc\max}$ and a modification of Eq. 1 for the
 166 critical shear stress. According to the deterministic design implemented in [6], the critical
 167 shear-stress is computed for θ_{cr} equal to 0.035 and using a stone diameter for which 67.5% of
 168 the stones (by weight) are retained in the sieving process ($D_{67.5}$). These changes are made to
 169 account for the fact that stones in a scour protection with smaller grading tend to move faster
 170 than those in a scour protection with a wide grading [6]. The maximum bed shear stress, in this
 171 case, is obtained from Eq. 5. The mean stone diameter D_{50} is related with $D_{67.5}$ by means of Eq.
 172 6, where D_{85} and D_{15} are defined in the same way as D_{50} and $D_{67.5}$ for the 15% and the 85%

173 percentiles. Then the minimum value of D_{50} is the one that complies with Eq. 7, noting that D_{50}
 174 depends on $D_{67.5}$, which is included in Eq. 1. Moreover, it must be noted that the wave- (τ_w) and
 175 current-induced bed shear stresses (τ_c) are dependent on the diameter D_{50} , which is used to
 176 calculate the bed roughness (k_s), assumed as $2.5D_{50}$ in the absence of ripples formation [14]. In
 177 the methodology presented by [6] no amplification factor is employed. Research showed that
 178 the design proposed by [6] led to smaller stone sizes when compared with the one proposed by
 179 [20]. In Eq. 5, 6 and 7, the bed shear stresses are expressed in N/m^2 .

180

$$181 \quad \tau_{wc\max} = 83 + 3.569 \times \tau_c + 0.765 \times \tau_w \quad (5)$$

182

$$183 \quad \log\left(\frac{D_{67.5}}{D_{50}}\right) = 0.25 \log\left(\frac{D_{85}}{D_{15}}\right) \quad (6)$$

184

$$185 \quad \tau_{cr}(D_{67.5}; \theta_{cr} = 0.035) > \tau_{wc\max} \quad (7)$$

186

187 *2.2 Dynamic scour protections*

188 In order to reduce even more the stone size required for scour protections in marine
 189 environment, innovative works have been performed aiming at dynamic scour protections,
 190 which allow the armour stones to move. The concept was primarily studied in [13] and later
 191 developed and extended by [3], [14] and [15]. The design methodology presented by [14] is
 192 still deterministic and mainly based on the definition of the damage number of the protection
 193 (S_{3D}). The damage number corresponds to a non-dimensional measure of the volume eroded
 194 per subzone of the scour protection defined as in [14].

195 The research performed by [14] presented an extensive set of 85 scour tests, including a
 196 physical model study at a Froude scale 1/50. This study proposed a formula (Eq. 8) to provide
 197 the predicted damage number (S_{3Dpred}),

198

$$199 \quad \frac{S_{3Dpred}}{N^{b0}} = a_0 \frac{U_m^3 T_{m-1,0}^2}{\sqrt{gd}(s-1)^2 D_{n50}^2} + a_1 \left(a_2 + a_3 \frac{\left(\frac{U_c}{w_s}\right)^2 (U_c + a_4 U_m)^2 \sqrt{d}}{g D_{n50}^2} \right) \quad (8)$$

200

201 where N is the number of waves in a storm, U_c is the average current velocity, s is the ratio
 202 between sediment's density (ρ_s) and water density (ρ_w), g is the gravitational acceleration, d is
 203 the water depth, U_m is the orbital bottom velocity and w_s is the sediments' fall velocity. $T_{m-1,0}$ is
 204 the energy spectral wave period, which for a JONSWAP spectrum, with $\gamma=3.3$ can be obtained
 205 from the peak period (T_p) as $T_{m-1,0}=1.107T_p$. In Eq. 8, b_0 , a_0 , a_2 and a_3 are equal to 0.243,
 206 0.00076, -0.022 and 0.0079, respectively. The constants a_1 (Eq. 9) and a_4 (Eq. 10) depend on
 207 the existence of following or opposed current (C) to waves (W). U_r stands for the Ursell
 208 number. D_{n50} is the nominal value of the mean stone diameter equal to $0.84D_{50}$. Regarding the
 209 number of waves in a storm, a value of 3000 waves was assumed. This was identified in [14]
 210 and [15] as the number of waves for which the damage number stabilises. However, the authors
 211 recognise that the minimum N for the S_{3D} to stabilise is yet to be fully understood, e.g. [24]
 212 performed physical model studies of wide-graded scour protections, concluding that damage
 213 still increased after 9000 waves. However, the damage increase reported in [24], for single
 214 layer wide-graded scour protections, might not be directly comparable to the type of damage in
 215 a scour protection with filter and armour layer tested in [14]. Regarding the latter, [12] noted
 216 that the rate of damage development is typically larger in the first 1000 waves and that between
 217 3000 and 5000 waves the damage development significantly decreases.

218

$$219 \quad a_1 = \begin{cases} 0 & \text{for } \frac{U_c}{\sqrt{gD_{n50}}} < 0.92 \text{ and } W \text{ following } C \\ 1 & \text{for } \frac{U_c}{\sqrt{gD_{n50}}} \geq 0.92 \text{ or } W \text{ opposed } C \end{cases}$$

220 (9)

221

$$222 \quad a_4 = \begin{cases} 1 & \text{for } W \text{ following } C \\ \frac{U_r}{6.4} & \text{for } W \text{ opposed } C \end{cases}$$

223 (10)

224

225 Eq. 8 provided close estimates of the actual damage number (S_{3Dmeas}) measured in the
 226 physical model. The reader is referred to [12], [14] and [15] for details on the physical model
 227 and the assessment of the measured damage number.

228 In [14] it was found that for S_{3D} between 0.25 and 1 there was movement of the armour layer
 229 stones without failure, i.e. dynamic stability was achieved. For S_{3D} below 0.25, no movements

230 occurred (statically stable scour protection). It was also reported that dynamic scour protections
 231 were obtained for $S_{3D} > 1$ (also see [12] and [15]). However, a transition zone was identified for
 232 $S_{3D} > 1$ in which dynamic profiles were developed in some cases and failure occurred in others.
 233 Therefore, a conservative limit of $S_{3D} \leq 1$ was proposed for the successful design of dynamic
 234 scour protections. The majority of the tests performed by [14] were done with a geotextile filter
 235 layer. However, in [12] it was found that dynamic scour protections based on the earlier study
 236 could be obtained when designing with a granular filter layer. One should note that the
 237 proposed limits for the damage number might not be applicable to wide-graded single layer
 238 scour protections, since such configuration was not tested in the original data [14] that led to
 239 the damage number formula, Eq. 8. Further research should be performed to address the
 240 damage behaviour on such type of protections, which are not addressed in the present research.
 241 According to the proposed design, the mean diameter of the armour stones is the one that
 242 complies with Eq. 11.

243

$$244 \left[a_0 \frac{U_m^3 T_{m-1,0}^2}{\sqrt{gd} (s-1)^2 D_{n50}^2} + a_1 \left(a_2 + a_3 \frac{\left(\frac{U_c}{w_s} \right)^2 (U_c + a_4 U_m)^2 \sqrt{d}}{g D_{n50}^{\frac{3}{2}}} \right) \right] N^{hb} \leq 1 \quad (11)$$

245

246 *2.3 Brief note about the deterministic design of scour protections*

247 There are several random variables included in the deterministic design of both static and
 248 dynamic scour protections. When calculating the bed shear-stress for static protections or the
 249 damage number for dynamic ones, it is crucial to define the values of the design wave height
 250 (H_d) and the associated wave period (T), which are used to determine the orbital bottom
 251 velocity (U_m). Moreover, the design current velocity (U_c) should also be addressed, among
 252 several other variables. The deterministic design of scour protections often uses the wave
 253 height associated to a specific return period (T_r), usually 50 years [6]. In the methodology used
 254 for static scour protections, [6] the authors calculate U_m for $H_{1/10}$, which refers to the mean
 255 wave height of the 10% highest waves in a sea state, for the location where the protection is
 256 going to be implemented. On the other hand, [14] uses the orbital bottom velocity calculated
 257 from the wave JONSWAP spectrum, with a peak enhancement factor of 3.3, defined by the
 258 $H_{1/3}$ and the peak period (T_p). The $H_{1/3}$ is analogous to $H_{1/10}$ but it refers to the 33.3%
 259 percentile. It is also often referred to as the significant wave height (H_s). The reader must note
 260 that despite H_s and $H_{1/3}$ are often assumed to be equivalent, they might be slightly different,

261 because H_s is directly obtained from the wave spectrum. In the present research, for the sake of
262 simplicity, one makes no distinction between these parameters, which is in agreement with the
263 procedure adopted in [3] when analysing static and dynamic scour protections. The energy
264 method was used to obtain H_s . However, for further details on the wave spectral parameters the
265 reference [3] is recommended.

266 Although the wave spectrum corresponds to a probabilistic short-term analysis of the sea state
267 characteristics, it does not represent a long-term probabilistic analysis. Hence, even when using
268 spectral analysis, these methodologies do not account for the long-term evolution of the design
269 wave height. Moreover, they do not include the long-term dependence between the wave
270 heights and the peak periods. Also the correlation between waves and current environment is
271 not taken into account. The present research did not focus on waves and current correlation.
272 However, recent works have been performed concerning this subject, e.g. in [25] a conditional
273 model is proposed to perform the joint model of waves and currents. It is concluded that the
274 joint behaviour of these variables produces differences in hydrodynamic loads estimation. In
275 [26] it is concluded that offshore standards tend to overestimate the ultimate limit state loads,
276 because they do not account for long-term correlation between waves and current environment.
277 The deterministic methodologies presented are also not able to consider the combined
278 variability of the environmental factors and the structural parameters of the protection, e.g. the
279 D_{50} , the uniformity parameter of the sediments, the density of the rock material or the
280 protection's thickness (see [3] for details on the structural parameters). However, in a
281 probabilistic design the simulation procedure enables the combination of different possible
282 values of these random variables. Therefore, a probabilistic design allows for the analysis of the
283 occurrence of failure in multiple loading scenarios combined with different characteristics of
284 the protection. However, it is important to note that such probabilistic analysis should be
285 performed within the limits of applicability of the methodologies used to predict damage
286 occurrence in scour protection [27].

287

288 **3. RELIABILITY ANALYSIS AND PROBABILISTIC DESIGN OF SCOUR** 289 **PROTECTIONS**

290 As stated before, the deterministic design of scour protections does not provide any probability
291 of failure related to the mean stone diameter used in the armour layer. Therefore, one is not
292 able to know how reliable the protection is, neither if the value of D_{50} is overestimated, namely
293 when using the methodology proposed by [20]. As a consequence, when innovative design

294 methodologies are proposed, as in [6] and [14], however, it is not possible to understand if the
 295 smaller size that is obtained complies with an acceptable level of safety when compared with
 296 the traditional design.

297 Probabilistic design and reliability assessment of scour protections is a key parameter in order
 298 to safely optimise the scour protection. Considering Eqs. 4, 7 and 11, one is able to define the
 299 failure criteria of static and dynamic scour protections according to Eqs. 12 and 13,
 300 respectively. These equations are referred to as limit state functions. Note that in Eq. 12, the
 301 amplification factor must be used if the maximum bed shear stress is calculated according to
 302 [20]. This equation also requires knowledge about the wave height and period, which are used
 303 to obtain the orbital bottom velocity that is required to calculate τ_{wcmax} , τ_w and τ_c . Details about
 304 this calculation are given in [6].

305

$$306 \quad f(\tau_{cr}; \tau_w; \tau_c) = \tau_{cr} - \tau_{wcmax} \quad (12)$$

307

$$308 \quad f(U_m; U_c; T_{m-1,0}; D_{50}; \rho_s; \rho_w; d; g; w_s) = 1 - S_{3Dpred} \quad (13)$$

309

310 If the limit state function $f(.)$ is lower than zero, then the failure of the scour protection occurs,
 311 either because the critical shear stress is exceeded or because the damage number of the
 312 protection exceeds the acceptable reference value for dynamic stability.

313 If one has a data record of the variables included in Eqs. 12 and 13, one may establish
 314 distributional models for the various variables and the limit state functions for different
 315 combinations of those variables can be simulated. The data record may correspond to hindcast
 316 or observed field data of wave heights and periods, current velocity, stone sizes, water depth or
 317 other variables. In practical situations, it is sometimes difficult to have a complete record of all
 318 variables. This is particularly evident for offshore locations and met-ocean data [28]. This often
 319 forces the designer to consider some of those variables as deterministic ones, e.g. ρ_w or ρ_s ,
 320 while the most important ones are analysed from a statistical point of view, e.g. H_d , T_p , U_m or
 321 U_c .

322 The reliability of the scour protection can be quantified by determining the probability of
 323 failure (P_f) of the protection. In the present research one considers this as the probability of the
 324 design criterion of the protection not being met. One can use Monte-Carlo simulations to

325 generate the random variables and compute the limit state functions. Then, for a large enough
326 number of simulations (n), the probability of failure (P_f) is provided according to Eq. 14.

327

$$328 \quad P_f = \frac{\#(f(X_i) < 0)}{n} = \frac{\sum_{i=1}^n I(f(X_i))}{n} \quad (14)$$

329

330 where X_i is the vector of random variables and $I(f(X_i))$ is an indicator function equal to 1 if
331 $f(X_i) < 0$ and equal to 0 otherwise. The number of times that $f(X_i) < 0$ is denoted by $\# f(X_i) < 0$. For
332 details on the minimum number of simulations (n) to obtain the stable value of P_f the reader is
333 referred to [29].

334 The results obtained from Eq. 14 provide the probability of failure for a certain mean diameter
335 of the armour stones. Furthermore, one can derive the probability associated to a range of mean
336 diameters, for specific design conditions, and then design the protection in a probabilistic
337 manner by choosing the value of D_{50} that corresponds to a certain admissible probability of
338 failure. In the following section a case study is addressed for which the deterministic and
339 probabilistic design is performed and discussed.

340

341 **4. CASE STUDY: SCOUR PROTECTION AT HORNS REV 3**

342 The met-ocean conditions at Horns Rev 3 offshore windfarm, fully available in [30], [31] and
343 [32], are used in order to illustrate how the reliability assessment of a scour protection and its
344 probabilistic design can be performed.

345 This offshore windfarm is under development and located in the Danish sector of the North Sea
346 (Figure 2), 20-35 km north-west of Blåvands Huk and 45-60 km from the city of Esbjerg. This
347 area is relatively shallow and the water depth ranges from 10 m to 20 m [30]. The local seabed
348 is dominated by non-cohesive sands [32]. The position for hindcast modelling corresponds to
349 the following coordinates: Latitude of 55.725°N and Longitude of 7.750°E. The available
350 database resulted in a total of 90 553 pairs of significant wave height and peak period. This
351 corresponded to an hourly output resolution for the period of 01-01-2003 to 01-05-2013, e.g.
352 124 months. The water depth at the referred coordinates was considered to be $d=18$ m.

353



Figure 2. Location of Horns Rev 3 offshore windfarm at the North Sea. [33].

354
355

356

357 The Conditional model, commonly used in offshore wind turbines design [34] was applied in
 358 order to simulate the significant wave height ($H_s=H_{1/3}$) and the peak period (T_p), which are
 359 further used to compute the variables included in Eqs. 12 and 13, e.g. U_m or $T_{m-1,0}$. For details
 360 on this model, the reader is referred to [35] or [36]. Regarding the methodology presented in [6]
 361 the value of $H_d=H_{1/10}$ is considered to be equal to $H_{1/10}=1.27H_s$, which is valid for the
 362 JONSWAP spectrum with a peak enhancement factor of 3.3. The conditional modelling
 363 approach is important as it enables one to obtain a model that allows for the variables
 364 extrapolation. One only has 10 years and 4 months of data. Thus, being possible that extreme
 365 events are not present in the dataset. The use of other models such as the ones based on copulas
 366 approach, e.g. [37] or normal transformations, e.g. [38], ultimately influences the probability of
 367 failure obtained. It is not the aim of the present paper to address this subject. However, the
 368 authors recognise that the analysis of this influence is also a knowledge gap in the literature
 369 concerning the reliability of scour protections. A review on possible statistical models for long-
 370 term analysis of H_s and T_p is given in [39].

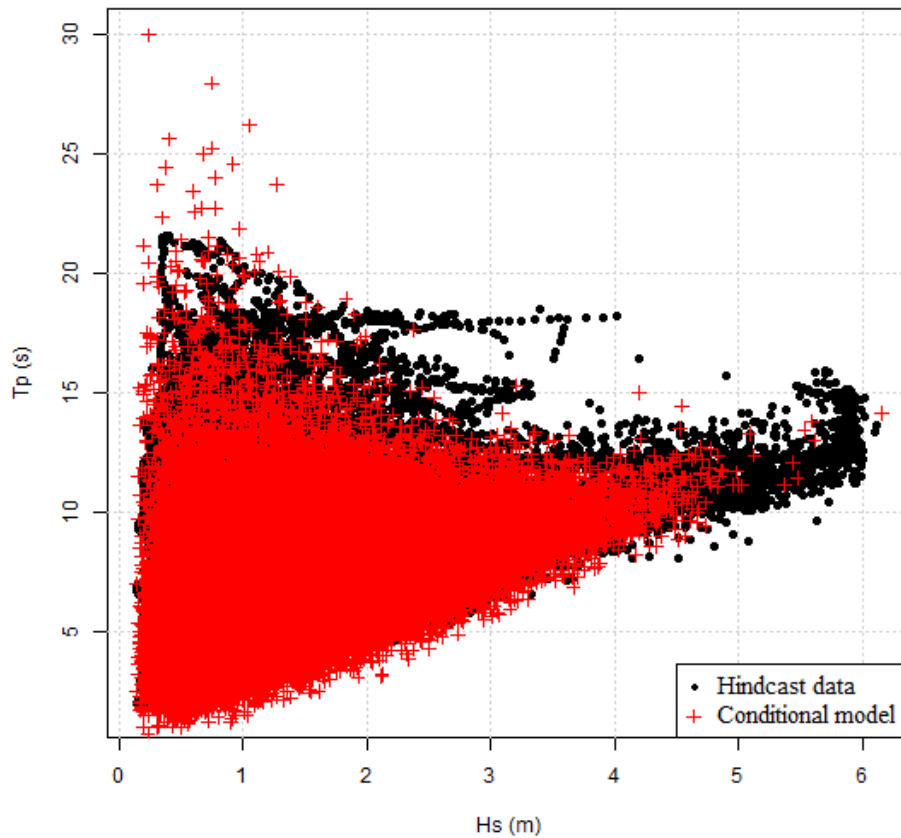
371 Regarding the relative comparison between the probabilities of failure given by each failure
 372 criteria, no influence from the actual model is expected since the same generated series are used
 373 to simulate the different limit state functions.

374 The hindcast data concerning H_s and T_p is provided in Figure 3, as well as a random sample of
 375 50 000 pairs of $(H_s; T_p)$ obtained from the Conditional Model. A visually good agreement is
 376 obtained between the sample and the generated data (Figure 3). The same generated samples of
 377 size n are used to simulate the limit state functions, when determining the probability of failure
 378 for the static and dynamic scour protections. It is important to note that when applying the
 379 conditional model, some of the generated values may fall outside the original range for which

380 the damage number formula, Eq. 8, was derived by [14]. For example, Figure 3 shows that
381 some of the smaller wave heights may present very large peak periods, e.g. 22 to 30 s.
382 However, it is unlikely that such pairs of H_s and T_p contribute to damage numbers that exceed
383 S_{3D} equal to 1. This occurs because, although the peak periods might be overestimated, the
384 significant wave height is not large enough to produce damage numbers above 1, according to
385 Eq. 8. Nevertheless, the future research should also be focused on the effects of the generation
386 model in the predicted damage numbers given according to [14], i.e. Eq. 8.

387 The statistical model, used to generate the random values of significant wave height and peak
388 period, will also affect the reliability assessment of the scour protection. For example, if
389 extreme wave heights (or periods) are underestimated, one may underestimate the probability
390 of failure associated to each criterion. Conversely, if the extreme wave heights (or periods) are
391 overestimated, the estimated probabilities of failure might be too conservative when compared
392 to the truthful (and unknown) value. Since the same model is used for all methodologies this
393 does not pose a problem in terms of the criteria comparison. However, it does influence the
394 assessment of each probability *per se*. Nevertheless, this remains as a problem of the model
395 fitting more than the methodology of reliability assessment discussed in the following sections.
396 Regarding this matter one must also note that the accuracy of the probabilities is also dependent
397 on the quality of the hindcast data, which in this case only has 10 years and 4 months.
398 However, for offshore locations the available data is often scarce and one has to fit the
399 statistical model to the records available, in spite of them being rather short.

400



401
 402 Figure 3. Hindcast data concerning the significant wave height and peak period at Horns Rev 3
 403 and random generated sample with $n=50\,000$ pairs of $(H_s; T_p)$.

404
 405 As a model simplification, the current velocity is considered independent from the wave height
 406 and the peak period. No time series were available for the current velocity (U_c). Based on the
 407 values reported in [30], this study considered that the current velocity followed a Weibull
 408 distribution, with an equivalent mean of 0.4 m/s and a standard deviation of 0.2 m/s. While the
 409 methodology presented in [20] considers different angles between U_c and the wave's direction,
 410 the methodology presented in [14] only considers unidirectional or opposing waves and
 411 currents. Therefore, a random angle of 0° and 180° was assigned to each simulation of the limit
 412 state functions. This is also a simplification of the present model but the authors recognise that
 413 improvements can be made if one considers a wider range of this angle. Nevertheless, this must
 414 be seen as a limitation of the criteria studied previously, more than a limitation of the reliability
 415 assessment proposed here. If concurrent directional wave and current data are available, it is
 416 possible to establish a probability distribution for the angle and simulate this accordingly. Note
 417 that the failure criteria influence the probability of failure, as shown in [27].

418 The water depth is also an important varying parameter that may influence the damage number
419 and the acting bed shear stress at the armour layer. However, in the present model and as a
420 simplification, this parameter was assumed to be deterministic variable in the process. At the
421 present stage of the research, a preference was given to the accurate model of the significant
422 wave height and the correlated values of the wave peak period. Nevertheless, it must be noted
423 that reductions in the water depth may lead to an increasing severity of the scour process on the
424 armour layer of the scour protection, eventually, contributing to reduce the reliability of a scour
425 protection, with the same thickness and the same mean stone diameter. On the other hand, the
426 water depth decrease may lead to limitations on the non-breaking wave heights at the
427 protection's location. Therefore, if the water depth is reduced one also has to account for the
428 effects on the wave's characteristics, which may difficult the straightforward identification on
429 the immediate effect on the damage number and the combined bed shear stress. To avoid a
430 possible bias on the interpretation of such effects from the water depth and the wave height, the
431 model was simplified to assume a constant water depth.

432 Horns Rev 3 windfarm is under development at the present date. However, [31] and [40]
433 suggest $D_{50}=0.4$ m or 0.35 m as possible mean stone diameters for the protection, respectively.
434 Moreover, in the present case study the following variables are analysed as deterministic,
435 according to the methodologies previously mentioned: the density of the rock material was
436 considered as $\rho_s=2650$ kg/m³, $N=3000$ waves, $\rho_w=1025$ kg/m³, $g=9.81$ m/s². The uniformity
437 parameter ($\sigma_U=D_{85}/D_{15}$) was defined as 2.5 as in [6]. In the following section the results
438 concerning the deterministic and the probabilistic design are presented and discussed. The
439 simulated values of H_s , T_p and U_c are provided from the conditional model fitted to the hindcast
440 data available for Horns Rev 3, as seen before.

441

442 **5. DESIGN RESULTS**

443 *5.1. Deterministic design of scour protections*

444 The deterministic design of scour protections typically uses the design wave height as the
445 significant wave height associated to a return period (T_R) of 50 years. In [30], the Peak Over
446 Threshold based on the Generalised Pareto distribution determined that, for this location, H_d
447 was equal to $H_{s50year}=6.7$ m. The concurrent wave peak period was calculated as for a
448 JONSWAP spectrum with a wave enhancement factor of $\gamma=3.3$, i.e. $T_p=4.4(H_s)^{0.5}=11.4$ s.
449 However, the hindcast data available concerns to 10 years and 4 months only. Therefore, one

450 should keep in mind that a considerable uncertainty is inherent to the estimated values for
451 $T_r=50$ years.

452 The design performed with [6] uses the mean wave height of the 10% highest waves in order to
453 calculate the orbital bottom velocity. Thus, U_m is calculated for $H_{1/10}=1.27H_{50\text{year}}=8.5$ m,
454 assuming a JONSWAP spectrum with a peak enhancement factor of 3.3. The methodology [14]
455 was applied with the significant wave height associated to $T_r=50$ years as in [20]. Both of these
456 methodologies use the peak period associated to the selected H_s . The orbital bottom velocity for
457 [6] is obtained with the linear wave theory, while in [14] is directly obtained from the wave
458 spectrum (also see [3]).

459 Table 1 provides the results for the deterministic design, which depends on the characteristic
460 values used to calculate the shear stress on the protection. Moreover, for the methodology
461 presented in [20], the mean diameter of the armour stones is calculated for several
462 amplification factors (α). A similar application is shown in [14]. One can see that the values
463 obtained in this case are similar to the ones reported for the referred deterministic design.

464 Table 1 shows that the innovative methodologies proposed by [6] and [14] lead to smaller
465 diameters when compared with the one obtained by the methodology from [20], which is more
466 conservative. This is a result of the different failure criteria that were selected and of the
467 different design values that were used. It is also possible to confirm that the dynamic scour
468 protection corresponds to the smallest stone size. In dynamic scour protections the difference
469 between the design for opposing waves and currents is not very noticeable, due to the small
470 mean current velocity ($U_c=0.4$ m/s). For large values of U_c , say 1-1.5 m/s, the differences in
471 D_{50} are larger, as shown in [3]. Nevertheless, the largest stone size given by [14] is associated
472 to waves opposing current. This is consistent with the fact that the damage number tends to be
473 larger for waves opposing currents than for waves following currents, as shown in [3] and [14].

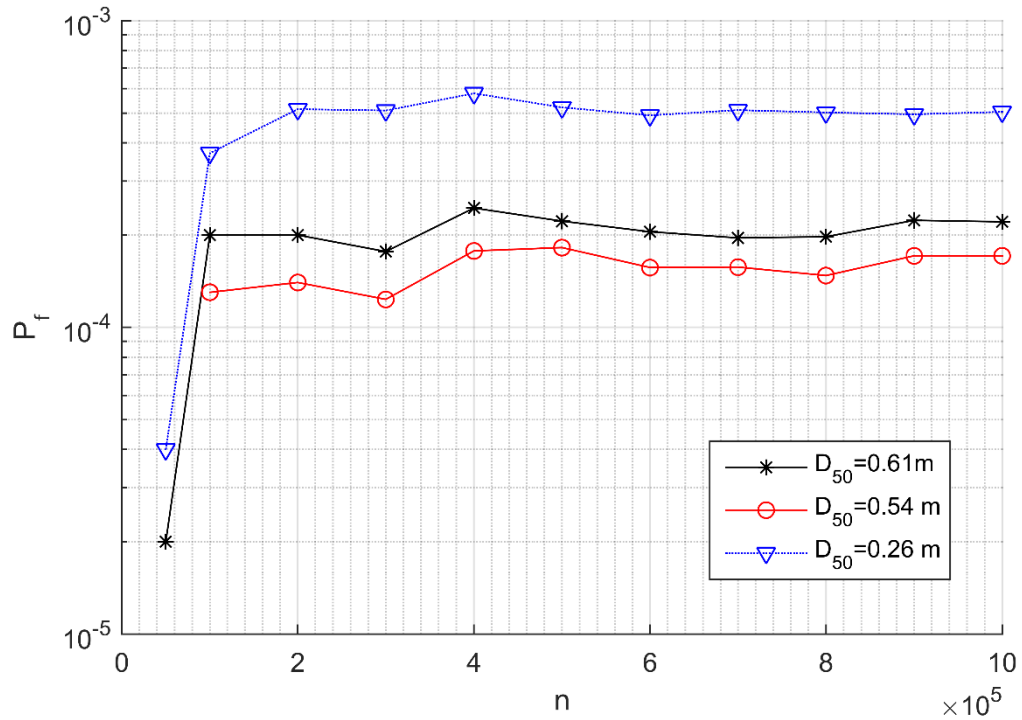
474 For a typical rip-rap scour protection, commonly placed with fall-pipe vessels [12], the
475 diameters given by the methodology in [20] for an amplification factor of 3 and 4 are rather
476 large. Moreover, the diameters obtained ($D_{50}=1.41$ m and $D_{50}=2.56$ m) are also very large when
477 compared with the size of rock material commonly used. Typical diameters of the armour
478 stones reported in the literature range from 0.15 m to 0.60 m depending on the site conditions
479 [7]. Table 1 provides acceptable diameters when compared to existent scour protections for
480 waves and currents combined, e.g. the offshore windfarms of Horns Rev 1 ($H_s=5.2$) and
481 Egmond aan Zee ($H_s=3.6$) use $D_{50}=0.40$ m. An extensive review of some design examples can
482 be found in [7] and [41]. The designs obtained by the methodologies from [6] and [14] seem

483 more appealing since the corresponding diameter of the stones is considerably smaller.
 484 Furthermore, the dynamic design of the scour protection enables one to use $D_{50}=0.26$ m, which
 485 is less than half of the size obtained by the methodology from [20] with $\alpha=2$.
 486 A question arises from Table 1: “Are the reduced diameters proposed by [6] and [14] as safe as
 487 those proposed by [20]?” In order to answer this question, the reliability of the proposed
 488 solutions is assessed. One considers that the wave height and the peak period are randomly
 489 generated from the Conditional model [35], while the mean current velocity follows the
 490 previously mentioned distribution. Random series of these variables were used to simulate the
 491 limit state functions, i.e. Eqs. 12 and 13. The probability of failure of each diameter was then
 492 calculated according to Eq. 14. The results are summarized in Figure 4 which presents the
 493 probability of failure as a function of the number of simulations performed.

494
 495

Table 1. Deterministic design of the scour protection at Horns Rev 3.

[20]			[6]			[14]		
Static Scour Protection			Static Scour Protection			Dynamic Scour Protection		
θ	0.056	[-]	θ	0.035	[-]	Direction	0;180	°
σ_u	2.5	[-]	σ_u	2.5	[-]	N	3000	waves
ρ_s	2650	[kg/m ³]	ρ_s	2650	[kg/m ³]	ρ_s	2650	[kg/m ³]
ρ_w	1025	[kg/m ³]	ρ_w	1025	[kg/m ³]	ρ_w	1025	[kg/m ³]
d	18	m	d	18	m	d	18	m
D_p	6.5	m	D_p	6.5	m	D_p	6.5	m
γ	3.3	[-]	γ	3.3	[-]	γ	3.3	[-]
H_s	6.7	m	H_s	6.7	m	H_s	6.7	m
T_p	11.4	s	T_p	11.4	s	T_p	11.4	s
U_c	0.4	m/s	U_c	0.4	m/s	U_c	0.4	m/s
U_m	$U_m(H_s;T_p)$	m/s	U_m	$U_m(H_{1/10};T_p)$	m/s	$U_m(H_s;T_p)$	$U_m(H_s;T_p)$	m/s
g	9.81	m/s ²	g	9,81	m/s ²	g	9.81	m/s ²
Result			Result			Result		
$D_{50}(\alpha=2)$	0.610		D_{50}	0.540	[m]	$D_{50}(0^\circ)$	0.250	
$D_{50}(\alpha=3)$	1.410	[m]						[m]
$D_{50}(\alpha=4)$	2.560					$D_{50}(180^\circ)$	0.260	



496

497 Figure 4. Probability of failure for each design methodology versus number of simulated values
498 of H_s , T_p and U_c .

499 Figure 4 shows that the methodology from [6] leads to the lowest probabilities of failure. The
500 values of the probability seem rather stabilised after $n=300\,000$. The probabilities are plotted in
501 the logarithmic scale. It is somehow counterintuitive that $D_{50}=0.54$ m yields a lower probability
502 of failure ($P_f=1.7 \times 10^{-4}$) than $D_{50}=0.61$ m ($P_f=2.2 \times 10^{-4}$). However, the failure criteria that leads
503 to those probabilities is different and as also noted by [27] the failure criteria does influence the
504 probability of failure. Therefore, the probability of failure must be understood as the chance of
505 a design criterion is not being met, under the random loading conditions given by H_s , T_p and
506 U_c . This means that $D_{50}=0.54$ has a smaller probability of not meeting the design criterion
507 given by [6], than the $D_{50}=0.61$ has of not meeting the design criterion given by [20].
508 Nevertheless, Figure 4 seems to indicate that both methodologies for static design lead to
509 diameters that have very similar probability of failure, i.e. the same probability that each design
510 criterion is not being respected. This suggests that the optimised solution provided by [6] not
511 only gave a smaller D_{50} than [20], but it seems to be within the same level of safety, i.e. P_f in
512 the order of 10^{-4} .

513 However, the reliability assessment was performed for an amplification factor of 2. Note that
514 several authors typically employ $\alpha=4$ in several design situations, e.g. [3], [42] or [43], which
515 means that those solutions tend to be more conservative than $D_{50}=0.61$ m. One can argue that

516 the curve given by [20] with $\alpha=2$ is not directly comparable to the curve given by [6]. As it will
 517 be discussed further, this argument is reasonable due to several differences between the static
 518 design criteria.

519 The probabilities associated to the methodology [14] are slightly larger than those obtained
 520 with the statically stable solutions from [6] and [20]. The $D_{50}=0.26$ m has $P_f=5\times 10^{-4}$. However,
 521 if one takes into consideration the variability and the uncertainty of the met-ocean environment,
 522 the values obtained might be considered acceptable in light of the substantial reduction of the
 523 mean stone diameter. An important aspect that can be noted is the consistency in the criteria
 524 provided by [6] and [14]. The design of a dynamic scour protection with a reduced diameter
 525 ($D_{50}=0.26$ m) gives a slightly larger probability of failure ($P_f=5\times 10^{-4}$) than the static scour
 526 protection ($P_f=1.7\times 10^{-4}$) with a larger mean diameter ($D_{50}=0.54$ m). Once again, note that the
 527 failure of both protections is analysed under different failure criteria. In the present case, it
 528 seems that a dynamic scour protection has a reliability level, which is in the same order as the
 529 static one designed according to [14], i.e. both of them in order of 10^{-4} . This is of great
 530 importance, because not only the size reduction may lead to lower costs of the scour protection,
 531 but it also minimizes the occurrence of other problems, e.g. the edge scour phenomenon, which
 532 increases for large stone diameters due to the sudden increase of the bed-roughness [44].

533 The results from Table 2 are somehow difficult to compare with other cases in the literature,
 534 because there is an evident lack of research performed on the reliability and safety assessment
 535 of scour protections analysed by means of the probabilities of failure. A reliability assessment
 536 of statically stable scour protections, designed according to [6], is presented by [11]. However,
 537 the authors do not consider the correlation effects between the significant wave height and the
 538 peak period. Moreover, H_p , T_p and U_c were assumed to follow Gaussian distributions. The
 539 minimum probability of failure obtained by [11] was in the range of 10^{-3} for a global safety
 540 factor of 1.5, defined as the ratio of the acting bed shear stress to the critical shear-stress. These
 541 values seem to indicate that the model chosen for the random variables considerably affects the
 542 probability of failure. Such evidence was also confirmed in studies related to other offshore
 543 components, e.g. in mooring lines by [45].

544

545 Table 2. Stabilized probability of failure calculated with the Conditional model model (124
 546 months).

Design Methodology	D_{50} [m]	P_f (n=1 000 000)
--------------------	--------------	---------------------

Static Scour Protection [20]	0.61	2.2×10^{-4}
Static Scour Protection [6]	0.54	1.7×10^{-4}
Dynamic Scour Protection [14]	0.260	5×10^{-4}

547

548 The scour protection at a monopile foundation consists of a system designed to mitigate scour
549 related failures. However, if the scour protection fails, the monopile is not expected to fail
550 immediately nor results in loss of human life (offshore wind turbines are unmanned structures).
551 In this sense, one could argue that probabilities of failure in the order of 10^{-4} might be
552 acceptable for the scour protection.

553 The probabilities of failure presented in Table 2 are computed based on a 124 months record.
554 Regarding the probability of failure in scour protections there is no guidance or obligatory
555 offshore standards to be followed, typically, in marine structures the annual probability of
556 failure may range from 10^{-3} to 10^{-6} , depending on the systems redundancy, the warning prior to
557 failure and the possibility of loss of life, e.g. see [46] and [47]. The values obtained for the
558 present design might be difficult to convert to equivalent annual values for a proper comparison
559 with the mentioned references. This is due to the fact that there is a dependence between the
560 sea-state conditions for each simulation, because one is using hourly data. Since the event from
561 hour (t_i) might be dependent from the event of hour (t_{i-1}), one is not able to assume a constant
562 rate of failure. Thus, the annual probability of failure will not be equal to the number of hours
563 in a year multiplied by the probabilities obtained in Table 2. Of course the time step used to fit
564 the joint model of H_s and T_p also leads to an influence in P_f . Regarding the comparative
565 analysis between criteria this does not pose a problem, because the same hourly data is used for
566 the three design situations. However, when trying to analyse the probability of failure
567 associated to extreme values, e.g. H_s associated to $T_r=100$ years or similar, the values of P_f are
568 not directly comparable with the ones being focused in this research.

569 The effects of the temporal resolution used to compute the probability of failure in offshore
570 engineering applications are analysed in [48]. Although favouring models, which are fitted to
571 annual maxima or clustered data, may lead to a better assessment of the extreme events, it must
572 be recognised that this may also lead to uncertainties when the records are rather short, as this
573 one with only 124 months. Nevertheless and as stated before, the main idea from the
574 comparison presented in Figure 4 and Table 2 is that the deterministic solutions seem to present
575 similar reliability measures. The authors recognise that further research considering other data

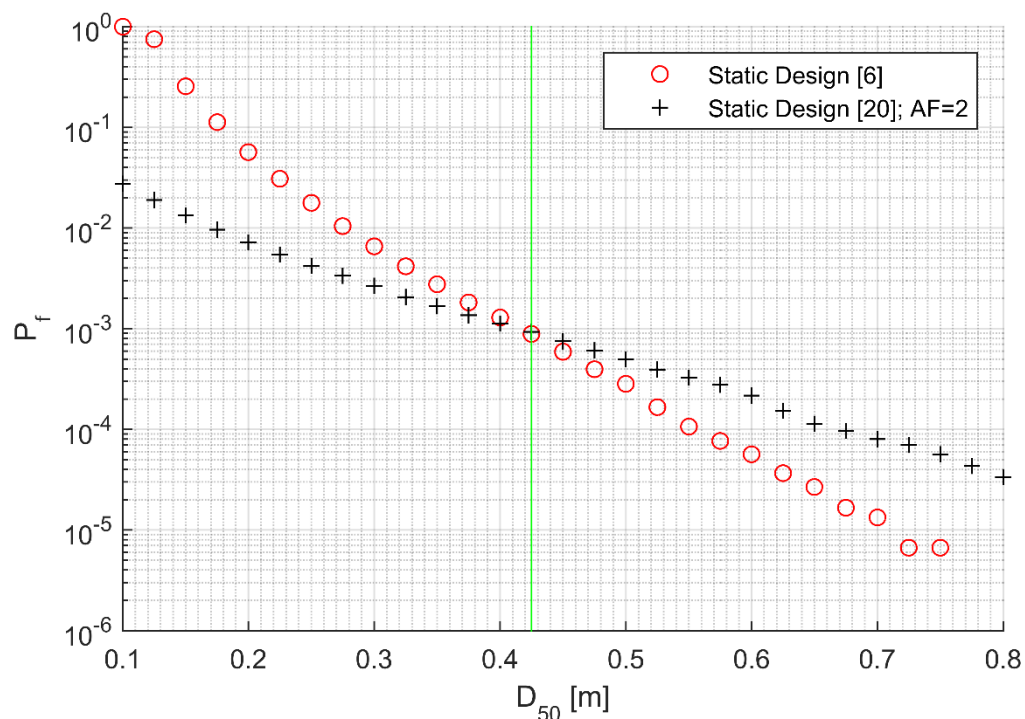
576 records and other temporal resolutions of H_s and T_p should be carried in order to properly
577 compare these probabilities of failure with the annual return period values currently employed
578 in structural design of offshore foundations.

579

580 5.2. Probabilistic design of scour protections

581 Instead of solely assessing the probability of failure of the scour protection, it might be relevant
582 to analyse the values of the mean stone diameter associated to a specific probability. This can
583 be performed by determining the relationship between D_{50} and P_f according to each
584 methodology.

585 In Figure 5, this relationship is established for the design of a static scour protection according
586 to the methodologies presented by [6] and by [20], with an amplification factor of 2 applied to
587 the latter. Results are obtained for a number of simulations set to 300 000, which is large
588 enough to ensure a stabilised value of the probability of failure (see Figure 4).



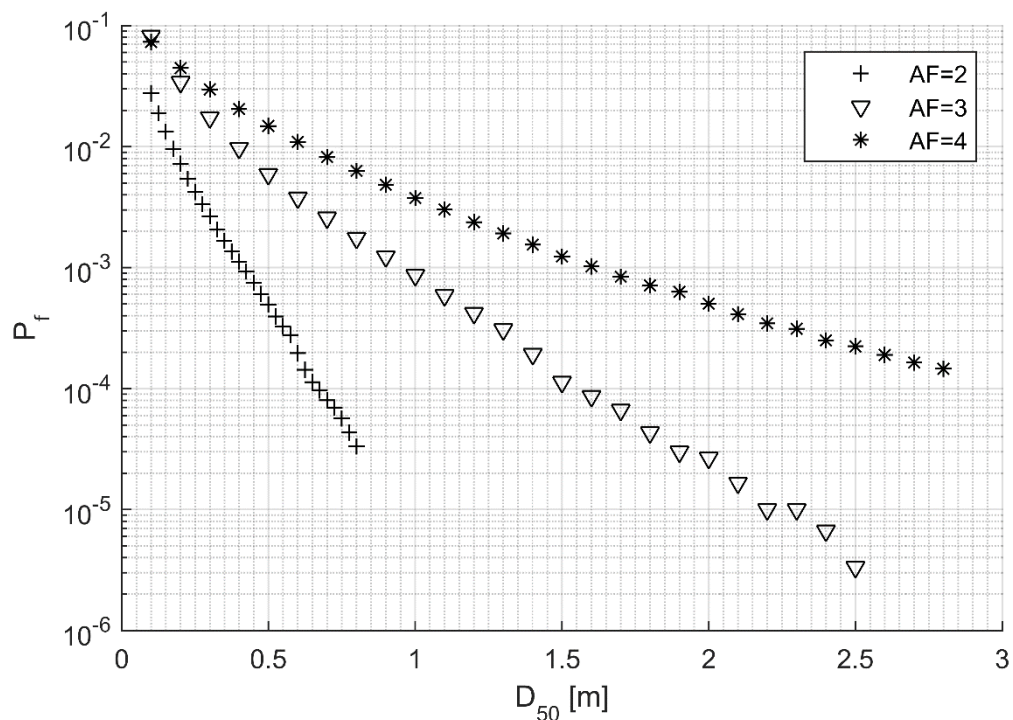
589

590 Figure 5. Safety comparison between static design criteria ($n=300\ 000$).

591

592 Figure 5 indicates there is a decrease of the probability of failure for increasing values of the
593 mean stone diameter, which is expected since larger diameters exhibit higher critical bed shear
594 stresses, therefore, being less likely to be dragged away from the armour layer. This behaviour
595 is in agreement with the results obtained by [11].

596 The deterministic design, previously presented, indicated that the methodology in [20] yielded
 597 more conservative sizes of the mean diameter. However, Figure 5, indicates that this
 598 methodology seems to be more conservative only for mean diameters larger than 0.42 m
 599 (vertical line in Figure 5). Conversely, as D_{50} decreases, the methodology in [20] yields smaller
 600 probabilities of failure than the methodology in [6]. Moreover, the methodology in [6] leads to
 601 a probability of failure of 1 for a mean diameter of 0.1 m, while according to the methodology
 602 in [20] the probability is much smaller, roughly 0.03. This difference points to a considerable
 603 uncertainty between both methodologies [6] and [20]. Such difference should be the aim of
 604 further research. Given these results, one may ask “are these two curves comparable?” i.e. can
 605 they be used to assess the same design situation? It is possible to argue that they are not since
 606 several different factors influence both criteria and may contribute for this somehow peculiar
 607 behaviour. Firstly, the results in Figure 5 considers an amplification factor of 2, which may not
 608 be the most reasonable choice for the waves and currents combined. As can be shown in Figure
 609 6, the probability of failure for the same mean stone diameter is highly dependent on the
 610 amplification factor, which is often determined by physical models adapted for a specific
 611 construction site.



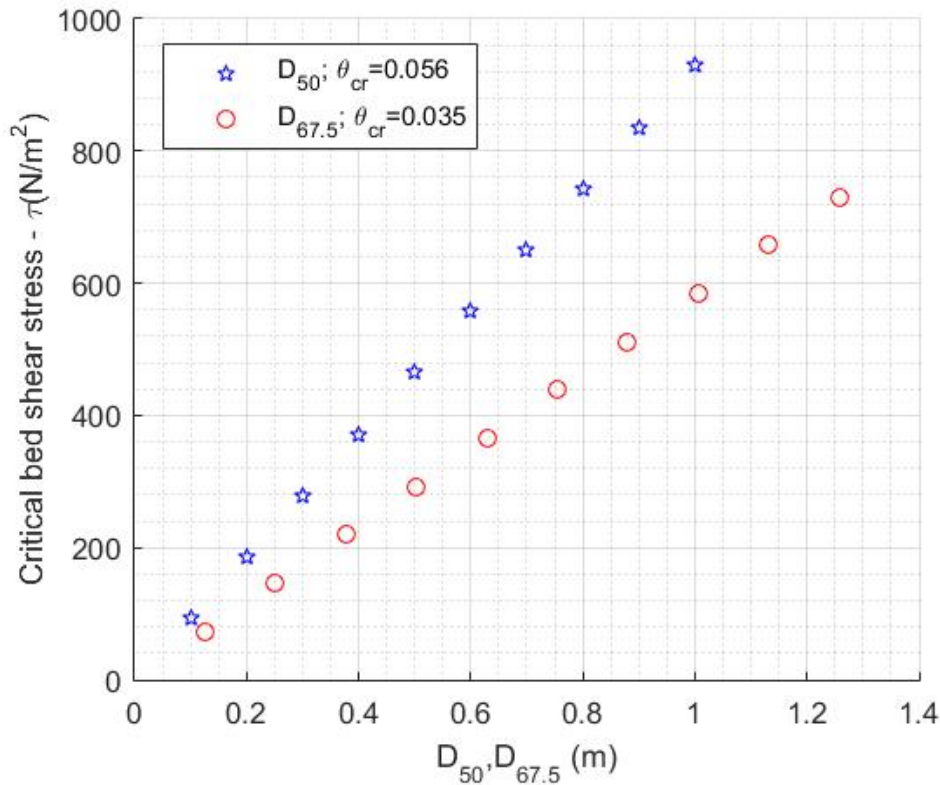
612
 613 Figure 6. Influence of the amplification factor in the probability of failure for the methodology
 614 in [20] ($n=300\ 000$).
 615

616 Figure 6 shows that when the amplification factor increases, a larger mean diameter must be
617 chosen to obtain the same probability of failure. This emphasises the fact that the methodology
618 proposed by [20] tends to be more conservative when the amplification factor is increased.
619 Nevertheless, the authors note that the definition of the amplification factor may represent a
620 drawback to the probabilistic design of static scour protections according to the methodology in
621 [20]. Although, several authors use $\alpha=4$, this value can be larger or smaller, depending on the
622 hydrodynamic conditions [18]. The fact that its evaluation is still assessed based on the
623 empirical knowledge of the designer, makes it harder to define standard values of α that should
624 be used to obtain the curve showed in Figure 5, which is intended to be comparable with the
625 methodology in [6]. The effect of the amplification factor on the probability of failure increases
626 for an increasing D_{50} .

627 In agreement with the deterministic design previously performed, Figure 6 shows that
628 amplification factors of 3 or 4 leads to very large mean stone diameters, which for a rip-rap
629 scour protection may not be a feasible material to be placed with the fall-pipe vessels, as
630 mentioned by [11].

631 Another aspect that may contribute to the behaviour showed in Figure 5 is the calculation of the
632 critical bed shear stress. Figure 7 shows the critical bed shear stress as a function of the
633 diameter of the stones. Note that, according to [6], the critical bed shear stress is calculated
634 with θ_{cr} equal to 0.035 and using the diameter $D_{67.5}$. On the other hand, the methodology in [20]
635 uses θ_{cr} equal to 0.056 and the mean stone diameter D_{50} . One can think about the critical bed
636 shear stress as being the resistance component of the limit state function (Eq.12). Figure 7
637 shows that, for smaller diameters, the difference between the resistance values obtained by both
638 methodologies is less significant. This difference becomes more relevant as D_{50} increases.
639 When the mean stone diameter increases, the resistance given by the methodology in [6] can be
640 seen to increase less than the resistance obtained by the methodology in [20] (Figure 7). This
641 should lead to larger probabilities given by the design according to [6] than according to in
642 [20]. However, this effect may be opposed by the different calculation of the acting bed-shear
643 stress which varies non-linearly with the increasing D_{50} .

644 Moreover, the non-linearity of the combined wave- and current-induced bed shear stress with
645 the variation of mean stone diameter may also contribute for the different behaviour between
646 the curves shown in Figure 5. Further research should be carried to fully address the influence
647 of this aspect. Note that the non-linear effects are mainly due to the influence of D_{50} on the
648 wave and current friction factors, as shown by [49] and [50].



650

651 Figure 7. Comparison of the critical bed shear stress calculated by the methods in [6] and [20].

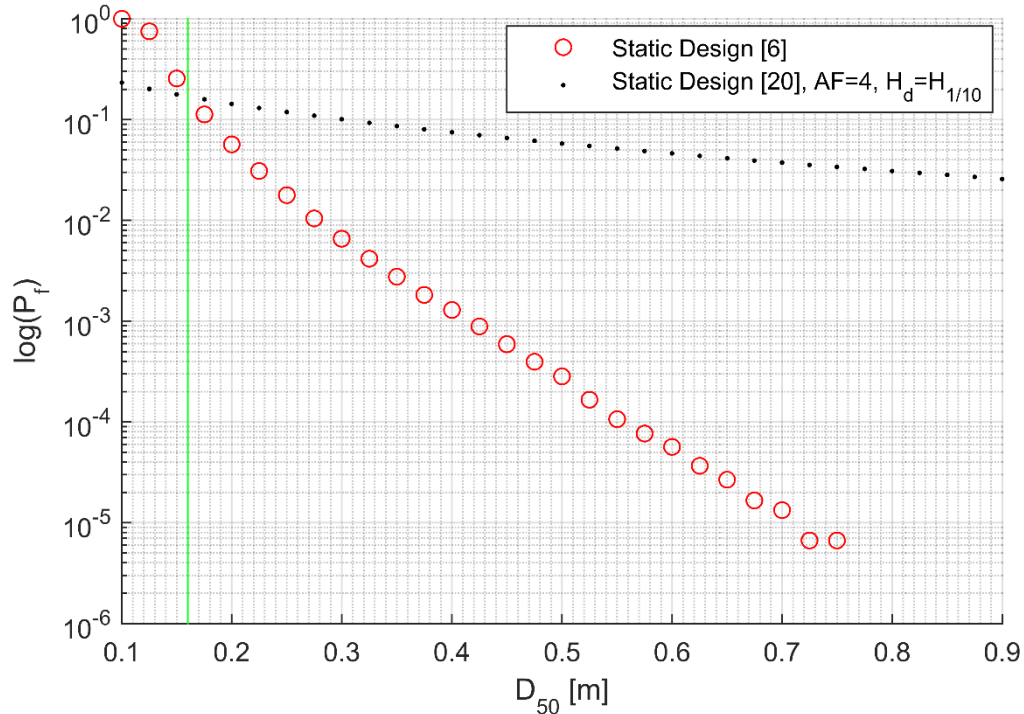
652

653 Finally, one must also note that the wave orbital bottom velocity (U_m) is calculated for the
 654 significant wave height (H_s) in the methodology in [20], while in the methodology in [6] it is
 655 calculated for the mean wave height of the top 10% of the waves ($H_{1/10}$). Therefore, the orbital
 656 bottom velocity used in [6] is more conservative than the one used in [20]. In non-cohesive
 657 sediments, as the ones studied in this case, research shows that the combined bed shear stress
 658 increases faster for smaller stone diameters, e.g. [3] and [6]. Therefore, when the diameter
 659 decreases, the effect caused by the different calculation of U_m may also contribute to the larger
 660 values of the probability of failure showed by the methodology in [6]. When the mean diameter
 661 increases, the effects associated to U_m dissipate and the methodology in [20] yields larger
 662 values of the probability of failure.

663

664 Figure 8 shows the probabilities of failure obtained with the methodology in [6] compared to
 665 those obtained with the methodology in [20] calculated with an amplification factor equal to 4
 666 and U_m calculated with $H_{1/10}$. As expected, the probabilities of failure for the methodology in
 667 [20] increase considerably since $U_m(H_s) < U_m(H_{1/10})$. For the sake of comparison, Figure 8 is
 limited to $D_{50}=0.9$ m, because the methodology in [20] only yields smaller probabilities of

668 failure for very large diameters (see Figure 6). In the case of Figure 8, it is possible to see that
 669 the intersection point between both methodologies occurs sooner than showed in Figure 5,
 670 close to $D_{50}=0.16$ m.
 671



672
 673 Figure 8. Influence of U_m in the probability of failure for the methodology in [20], compared
 674 with the standard application of the methodology in [6] ($n=300\,000$).
 675

676 These results show that, for static scour protections, it might be difficult to select a D_{50} for a
 677 pre-defined probability of failure. Nevertheless, in the present case study, for probabilities of
 678 failure smaller than 10^{-3} , the methodology in [6] consistently leads to smaller mean stone
 679 diameters (see Figure 5 and Figure 6). In practical situations, it is recommended that both
 680 curves are established and analysed before selecting the design value of D_{50} . Moreover, it is
 681 also noted that selecting D_{50} may also depend on factors such as the available material, the
 682 transportation cost and the construction technique (e.g. fall-pipe vessels, cranes, lifters), which
 683 may lead the designer into avoiding the use of very large diameters, e.g. above 0.8 m.

684 When designing a dynamic scour protection, it is important to establish the relation between the
 685 stone diameter and the probability of failure for the criterion presented in [14]. Moreover, since
 686 the methodology presented in [14] is an improvement of the method for static scour protections
 687 proposed in [6], it is also important to understand if both criteria provide an equivalent safety

688 level, i.e. is there a relation between a static scour protection designed with a certain D_{50} and a
689 dynamic scour protection designed with a reduced D_{50}^* , for any $D_{50}^* < D_{50}$.

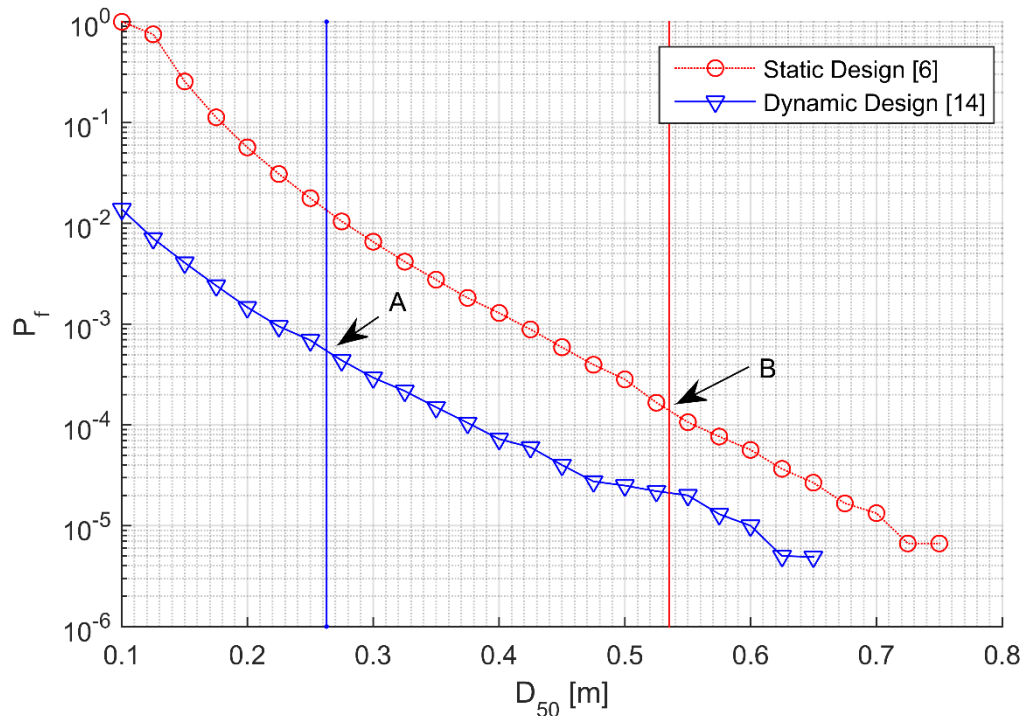
690 Figure 9 presents the comparison of both methodologies for the case study introduced in the
691 previous section. For the tested range of mean stone diameters, it can be seen that the criterion
692 proposed by the static design consistently leads to larger probabilities of failure for the same
693 mean stone diameter. This is expected since the dynamic design allows for the movement of the
694 stones, which means that smaller diameters can be used in the design without considering that
695 failure occurs. However, a fair comparison between criteria must be performed for different
696 diameters, i.e. the one used for a static design and the reduced one used in the dynamic design.

697 Point A (0.26 m; 5×10^{-4}) and Point B (0.54 m; 1.7×10^{-4}) in Figure 9 correspond to the
698 deterministic design values previously presented for the dynamic and static scour protections,
699 respectively. As seen before, these two points show that the probability of failure is larger for
700 the reduced diameter D_{50}^* . However, one is able to see that other values of D_{50} could be used,
701 smaller than $D_{50}=0.54$ m but larger than 0.26 m, still yielding probabilities of failure which are
702 are in the order of 10^{-4} . For example, if the designer is not comfortable with using a $D_{50}^*=0.26$
703 m, he may still use, for instance, a $D_{50}=0.45$ m, which yields a value of P_f in the order of 10^{-5}
704 for the dynamic criteria and 10^{-4} in the static one, but still represents a smaller mean diameter
705 when compared with the one required for static stability, i.e. $D_{50}=0.54$ m. In this sense, and for
706 design purposes, one is now able to select the mean stone diameter for a pre-defined probability
707 of failure from the curves showed in Figure 9.

708 Figure 9 shows that, depending on the level of safety, i.e. for the same probability of failure, the
709 “static mean stone diameter” can be approximately reduced by 10 to 15 cm if one uses a
710 “dynamic mean stone diameter”. This is of great importance as, for the present case study, it
711 helps to validate that a solution based on a dynamic scour protection yields a similar level of
712 reliability as the one based on the static design. Furthermore, it enables the designer to
713 understand how the proposed reduction in the diameter is influencing the safety level according
714 to the statically stable or dynamically stable criteria. Eventually, the designer may adopt an
715 intermediate solution between both diameters and he is still optimising the dimension of the
716 protection when compared with the traditional static design.

717 As seen when dealing with the reliability assessment of the deterministic design approach, the
718 authors note that further research should be performed in order to generalize this procedure for
719 other case studies. The lack of research addressing the probabilistic design of scour protections
720 for offshore wind turbines leaves space to improve these results and to compare them with

721 different design conditions. However, the confidential policies concerning data sharing, design
722 procedures and the occurrence of failures in the offshore wind industry do not facilitate the
723 increase in the number of case studies to be analysed. Therefore, only a confined group of
724 people has experience and knowledge to design scour protections [6]. Nevertheless, the
725 successful development of physical model studies concerning dynamic scour protections, e.g.
726 [12], [13], [14] and [15], as well as the consistent levels of safety that were identified for the
727 present case study justify the need for further research on the matter as a possible way to
728 optimise the design of scour protections.
729



730
731 Figure 9. Probabilities of failure as a function of the mean stone diameter, comparison between
732 static [6] and dynamic design [20].
733

734 **CONCLUSIONS**

735 A methodology to perform the reliability assessment and the probabilistic design of static and
736 dynamic scour protections was performed by means of a case study. The research was based on
737 the met-ocean data available for Horns Rev 3 offshore windfarm. For the considered case
738 study, it was concluded that it is possible to design a dynamic scour protection, according to
739 [14], with a similar reliability of a static scour protection designed according to [6]. Moreover,
740 both design methodologies showed that the reduction of the mean diameter, from a static

741 stability towards a dynamic stability, may be used for practical purposes. One is able to use a
742 mean diameter between the statically stable and the dynamically stable one within the same
743 order of the probability of exceeding the design criterion.

744 It was also concluded that further research should be carried in order to properly address the
745 comparison between the probabilistic design made with the methodology [6] and [20]. It was
746 found that the probability of failure was considerably influenced by the amplification factor, the
747 Shields critical parameter, the diameter used to compute the critical bed shear-stress and the
748 calculation of the orbital bottom velocity. The design options made regarding these aspects may
749 invalidate a straight comparison between the criteria adopted by [6] and [20]. Nevertheless, for
750 probabilities smaller than 10^{-3} , regardless of the amplification factor the methodology [20]
751 tended to provide larger mean diameters than the methodology [6]. However, it is advisable to
752 perform the reliability assessment for several values of the amplification factor, so that the
753 design decisions are better informed. Also the proposed design should always be validated by
754 means of physical model studies, as it is common in scour protection studies, e.g. [11] and [15].
755 The findings of this paper suggest that in practical situations one should calculate the
756 relationship between the mean stone diameter and the probability of failure for several
757 methodologies, in order to make an informed design decision. Moreover, the analysis of the
758 influence of the time resolution of the records of H_s and T_p on the probabilities obtained
759 remains to be fully understood. Further research should address this aspect, since typical
760 guidelines for structural design are referred to annual values. The influence of the statistical
761 model used to generate correlated wave heights and periods, as well as the correlation between
762 the sea-state and the current velocity, are also key aspects to improve the accuracy of reliability
763 analysis applied to scour protections. Finally, it should also be noted that the reliability analysis
764 based on different design criteria and the possible probabilistic design require a clear definition
765 on the general rules that define the required protection's safety level, which are yet not found in
766 the literature and should be the aim of future research.

767

768 **ACKNOWLEDGEMENTS**

769 T. Fazeres-Ferradosa is funded by the Portuguese Foundation for Science and Technology
770 (FCT) under the Ph.D. scholarship PB/BD/113454/2015 – Doctoral Program INFRARISK. T.
771 Fazeres-Ferradosa acknowledges Dr. Francisco Q. Fazeres (ULSAM) on the enlightening
772 discussions on survival and reliability analysis.

REFERENCES

- [1] WindEurope, “The European Offshore Wind Industry: key trends and statistics 2016,” WindEurope, Brussels, 2017.
- [2] L. Prendergast, K. Gavin and P. Doherty, “An investigation into the effect of scour on the natural frequency of an offshore wind turbine,” *Ocean Engineering*, vol. 101 (1), pp. 1-11, 2015.
- [3] L. De Vos, “Optimisation of Scour Protection Design for Monopiles and Quantification of Wave Run-Up - Engineering the Influence of an Offshore Wind Turbine on Local Flow Conditions - PhD Thesis,” University of Ghent, Ghent, 2008.
- [4] M. B. Zaaijer and J. Tempel, “Scour Protection: A Necessity or a Waste of Money?,” in *Proceedings of the 43th IEA Topical Expert Meeting*, Stockholm, 2004.
- [5] R. Whitehouse, *Scour at marine structures: A manual for practical applications*, London: Institution of Civil Engineers, 1998.
- [6] L. De Vos, J. d. Rouck, P. Troch and P. Frigaard, “Empirical design of scour protections around monopile foundations. Part 1: Static approach,” *Coastal Engineering*, vol. 58, pp. 540-553, 2011.
- [7] C. Matutano, V. Negro, J.-S. López-Gutiérrez and M. D. Esteban, “Scour prediction and scour protections in offshore wind farms,” *Renewable Energy*, vol. 57, pp. 358-365, 2013.
- [8] S. Bhattacharya, “Challenges in Design of Foundations for Offshore Wind Turbines,” *Engineering and Technology Reference*, pp. 1-9, 2014.
- [9] A. Gonzalez-Rodriguez, “Review of offshore wind farm cost components,” *Energy for Sustainable Development*, pp. 10-19, 2017.
- [10] J. H. den Boon, J. Sutherland, R. Whitehouse, R. Soulsby, C. J. M. Stam, K. Verhoeven, M. Høgedal and T. Hald, “Scour behaviour and scour protection for monopile foundations of offshore wind turbines,” in *European Wind Energy Conference & Exhibition*, London, UK, 2004.
- [11] T. Fazerer-Ferradosa, F. Taveira-Pinto, L. d. Neves and M. T. Reis, “Design of Scour Protections and Structural Reliability Techniques,” in *Sustainable Hydraulics in the Era of Global Change, Chapter 85*, Liege, CRC Press, Print ISBN 978-1-138-02977-4, DOI: 10.1201/b21902-91, 2016, p. 527–532.
- [12] P. Schoesitter, S. Audenart, L. Baelus, A. Bolle, A. Brown, L. d. Neves, T. Fazerer-Ferradosa, P. Harens, F. Taveira-Pinto, P. Troch and R. Whitehouse, “Feasibility of a dynamically stable rock armour layer scour protection for offshore wind farms,” in *International Conference on Ocean, Offshore and Arctic Engineering*, San Francisco, California, 2014.
- [13] E-Connection, Vestas Wind Systems D.K. Germanischer Lloyd Windenergie D, “OPTI-PILE, Fifth Research and Technological Development Framework,” 2002-2004.
- [14] L. De Vos, J. De Rouck, P. Troch and P. Frigaard, “Empirical design of scour protections around monopile foundations - Part 2 - Dynamic approach,” *Coastal Engineering*, vol. 60, pp. 286-298, 2012.
- [15] R. Whitehouse, A. Brown, S. Audenaert, A. Bolle, P. Schoesitter, P. Haerens, L. Baelus, P. Troch, L. d. Neves, T. Fazerer-Ferradosa and F. Taveira-Pinto, “Optimising scour protection stability at offshore foundations,” in *Proceedings of the 7th International Conference on Scour and Erosion*, Perth, Australia, 2014.
- [16] J. Fredsøe and R. Deigaard, *Mechanics of Coastal Sediment Transport - Advanced Series on Ocean Engineering*, vol 3, Singapore: World Scientific, 1992.
- [17] B. Melville and S. Coleman, *Bridge Scour, USA - Colorado*: Water Resources Publications, 2000.
- [18] B. M. Sumer and J. Fredsøe, *The Mechanics of Scour in the Marine Environment*, Singapore: World Scientific, 2002.
- [19] A. Agrawal, M. Khan and Z. Yi, “Handbook of Countermeasures Designs - report No FHWA-NJ-2005-027,” New Jersey Department of Transportation & Federal Highway Administration US Department of Transportation Washington D.C., 2007.
- [20] R. Soulsby, *Dynamics of marine sands: a manual for practical applications*, Thomas Telford, 1997.
- [21] A. F. Shields, “Application of similarity principles and turbulence research to bed-load movement, vol 26,” *Mitteilungen der Preussischen Versuchsanstalt für Wasserbau und Schiffbau*, pp. 5-24, 1936.
- [22] R. Soulsby and S. Clarke, “Bed Shear-Stresses Under Combined Waves and Currents on Smooth and Rough Beds. Report TR 137,” HR Wallingford, UK, 2005.
- [23] J. Malarkey and A. Davies, “A simple procedure for calculating the mean and maximum bed stress under

- wave and current conditions for rough turbulent flow based on Soulsby and Clarke's (2005) method," *Computers & Geosciences*, vol. 43, pp. 101-107, 2011.
- [24] A. Schendel, N. Goseberg and T. Schlurmann, "Experimental study on the performance of coarse grain materials as scour protection," in *Coastal Engineering Proceedings - 34th International Conference on Coastal Engineering*, Seoul, 2014.
- [25] K. Bruserud, S. Haver and D. Myrhaug, "Joint description of waves and currents applied in a simplified load case," *Marine Structures*, vol. 58, pp. 416-433, 2018.
- [26] K. Bruserud and S. Haver, "Waves and associated currents—experiences from 5 years metocean measurements in the northern North Sea," *Marine Structures*, vol. 2, p. In Press, 2017.
- [27] T. Fazerer-Ferradosa and F. Taveira-Pinto, "Pre-assessing the feasibility of a design performance function for scour protection systems in offshore foundations," in *Conference Proceedings of the 36th IAHR World Congress*, The Hague, 2015.
- [28] E. Vanem, "Uncertainties in extreme value modelling of wave data in a climate change," *Journal of Ocean Engineering and Marine Energy*, pp. 339-359, 2015.
- [29] F. Fajardo, J. Perez, M. Alsina and J. R.-. Marques, *Simulation Methods for Reliability and Availability of Complex Systems*, New York: Springer, 2010.
- [30] DMI, "Horns Rev 3 Offshore Wind Farm - Metocean," DMI - Danish Meteorological Institute & Orbicon A/S, Copenhagen, Denmark, 2013.
- [31] Energinet, "Horns Rev 3 Offshore Wind Farm - marine mammals - technical report 043," Energinet, Orbicon A/S, BioConsult SH GmbH & Co.KG, Denmark, 2014.
- [32] H. Kristensen, H. L. B. Gurieff, J. Steer and N. Richard, "Horns Rev 3 Results Report - Geo investigation 2012," Rambøll og Energinet, 2013.
- [33] S. Rodrigues, C. Restrepob, E. Kontos, R. T. Pinto and P. Bauer, "Trends of offshore wind projects," *Renewable and Sustainable Energy Reviews*, vol. 49, p. 1114–1135, 2015.
- [34] DNVGL, "DNV Recommended Practice C205 - Environmental Loads and Conditions," Det Norsk Veritas AS, Norway, 2017.
- [35] E. Bitner-Gregersen, "Joint met-ocean description for design and operation of marine structures," *Applied Ocean Research*, pp. 279-292, 2015.
- [36] E. M. Bitner-Gregersen and S. Haver, "Joint Environmental Model for Reliability Calculations," in *Proceedings of the 1st International Offshore and Polar Engineering Conference*, Edinburgh, United Kingdom, 1991.
- [37] E. Vanem, "Joint statistical models for significant wave height and wave period in a changing climate," *Marine Structures*, vol. 49, pp. 180-205, 2016.
- [38] C. Lucas and C. Guedes-Soares, "Bivariate distributions of significant wave height and mean wave period of combined sea states," *Ocean Engineering*, vol. 106, pp. 341-353, 2015.
- [39] P. Jonathan and K. Ewans, "Statistical Modelling of extreme ocean environments for marine design: A review," vol. 62, pp. 91-109, 2013.
- [40] Vattenfall, "corporate.vattenfall.dk," 2017. [Online]. Available: https://corporate.vattenfall.dk/globalassets/danmark/vores_vindmoller/horns_rev_3/hr3_nyhedsbrev_01.pdf. [Accessed 11 01 2018].
- [41] R. Whitehouse, J. Harris, J. Sutherland and J. Rees, "The nature of scour development and scour protection at offshore windfarm foundations," *Marine Pollution Bulletin. Volume 62. Issue 1*, pp. 73-88, 2011.
- [42] G. Hoffmans and H. Verheij, *Scour Manual*, Rotterdam: CRC Press, 1997.
- [43] A.C.Z., Van Oord, "Scour Protection for 6 MW OWEC with Monopile Foundation in North Sea," Gorinchem, 2003.
- [44] T. Petersen, B. Sumer, J. Fredsøe and J. Schouten, "Edge scour at scour protections around piles in marine environment - Laboratory and field investigation," *Coastal Engineering*, vol. 106, pp. 42-72, 2015.
- [45] R. Montes-Iturrizaga and E. Heredia-Zavoni, "Reliability analysis of mooring lines using copulas to model statistical dependence of environmental variables," *Applied Ocean Research. vol. 59.*, pp. 564-576, 2016.
- [46] DNV, "Classification Notes. N30.6 - Structural Reliability Analysis of Marine Structures," Det Norske Veritas, 1992.
- [47] DNVGL, "DNVGL - ST- 0262 - Lifetime extension of wind turbines," Det Norske Veritas AS, Norway, 2017.

- [48] S. Winterstein, G. Kleiven and O. Hagen, "Comparing extreme wave estimates from hourly and annual data," in *Proceedings of the International Offshore and Polar Engineering Conference*, Stavanger, Norway, 2001.
- [49] R. Simons, T. J. Grass, W. Saleh and M. M. Tehrani, "Bottom shear stresses under waves with a current superimposed," in *24th International Conference on Coastal Engineering*, Kobe, Japan, 1994.
- [50] A. Roulund, J. Sutherland, D. Todd and J. Sterner, "Parametric equations for Shields parameter and wave orbital velocity in combined current and irregular waves," in *Proceedings of the 8th International Conference on Scour and Erosion*, Oxford, UK, 2016.

775

776

777

778